The classical Schrödinger equation

The classical Schrödinger equation

Bogdan Mielnik†‡ and Marco A Reyes†

† Departamento de Física, Centro de Investigación y Estudios Avanzados del IPN, Apdo. Postal 14-740, México DF 07000, México
‡ Department of Physics, Warsaw University, Warsaw, Poland

Abstract. Prüfer's spectral algorithm is applied to the classical analogue of Schrödinger's equation. The discrete spectrum is interpreted as a bifurcation phenomenon caused by two simultaneous classical motions: rotation and squeezing. The energy eigenvalues coincide with the bifurcation parameters for the classical orbits.

1. Introduction

One of the known curiosities of the one-dimensional Schrödinger equation is its reducibility to the first-order differential equation of Riccati. Given the eigenvalue problem for Schrödinger's wavepacket $\psi(x)$:

$$-\frac{1}{2}\frac{d^2}{dx^2}\psi(x) + [V(x) - E]\psi(x) = 0 \tag{1}$$

(where $m = \hbar = 1$), the formal substitution

$$\psi(x) = e^{\phi(x)} \tag{2}$$

leads to the classical Riccati equation for $f(x) = \phi'(x)$:

$$f'(x) + f(x)^2 = 2[V(x) - E]. \tag{3}$$

Despite its apparent simplicity, (3) is one of the non-trivial and persistently returning problems in mathematical physics. In fact, even the field equations of general relativity might be viewed as an 'analogue' of the Riccati equation (see e.g. [1]). An obvious idea would be to replace completely the spectral problem (1) by its first-order equivalent (3). The difficulties, though, are formidable. In the first place, the ansatz (2) is impractical if $\psi(x)$ is a real sign changing function. Moreover, (3) has a tendency to create singularities of $f(x)$, which appear even for $V(x) = $ constant, and correspond to the nodal points of $\psi(x)[V(x) \equiv V_0 \Rightarrow f(x) = -k\tan(kx)$, where $k = \sqrt{2(E - V_0)}]$. The subtler ansatz of Aharonov and Au [2] takes care only of a part of this difficulty.

A different chapter in these attempts was opened by the angular analogues of the Riccati equation (3) studied by Prüfer [3], Milne [4], Drukarev [5] and Francetti [6]. Yet their works appeared at the wrong time (or in the wrong place?) and did not receive the attention which they deserved. The methods of Prüfer and Milne [3, 4] were soon overshadowed by the (less precise) WKB [7]. Drukarev and Francetti, apparently, have formulated their equations just to facilitate the calculation of the phase shifts (which they did, but the achievement later faded together with the whole 'phase shift trend'). As a result, the multiple forms of

the Riccati equation remain a kind of sophisticated curiosity, basically known but seldom applied. Notable exceptions are the techniques of evaluating the number of energy levels for one-dimensional Schrödinger's operator [8–11], developed in the classical works of Calogero [12, 13]. Yet the capacities of the method to determine the energy spectra are far from exhausted. Our purpose here is to complete the story, by studying the exact numerical consequences of the angular algorithms [3–6]. We shall show that their numerical integration is, most likely, one of the most powerful approximate methods to determine the eigenvalues of one-dimensional (or spherical) spectral problems, which might reduce the traditional perturbation calculus, at least for one-dimensional eigenvalue problems, into a kind of museum piece. What is no less interesting is that the method suggests a new concept of the spectrum, which might exceed the limits of the linear theory.

2. The classical model of Schrödinger's equation

Curiously, the meaning of the algorithm is best seen by forgetting completely about the quantum mechanical sense of Schrödinger's equation and sticking to its classical equivalent. This point of view, though seldom applied, has some notable traditions (see e.g. discussions in the 1970s [14], the works on the shooting method, discussions by Coleman [15] and by Ashtekar [16]). Its most provocative expression was the description of the Saturn rings as the band spectrum of Schrödinger's operator [17].

To perceive the classical sense of (1) denote the variable x by t and call it *time*; put also $q = \psi(t)$, $p = \psi'(t)$. Equation (1) then becomes

$$\frac{dq}{dt} = p \qquad \frac{dp}{dt} = 2[V(t) - E]q. \tag{4}$$

Note, that (4) coincides with the canonical equations for the pair of classical variables q, p defined by a time-dependent Hamiltonian

$$H(t) = \frac{p^2}{2} + [E - V(t)]q^2 \tag{5}$$

representing the classical oscillator with a time-dependent quadratic potential $V(q, t) = [E - V(t)]q^2$. The classical phase space trajectory of (4), (5):

$$\mathbf{q}(t) = \left\| \begin{matrix} q(t) \\ p(t) \end{matrix} \right\| (t \in \mathbf{R}) \tag{6}$$

'paints' a detailed image of Schrödinger's wavefunction $\psi(x)$ and its first derivative $\psi'(x)$. This fact has been decisive in representing the spectral bands of Schrödinger's operator as the stability bands of a classical system (the Saturn rings! [17]). It is as useful in analysing the point spectra.

3. The bifurcations

Assume for simplicity that none of E, $V(t)$ is positive, and $V(t)$ vanishes outside of a finite interval $[a, b] \in \mathbf{R}(V(t) = 0$ for $t < a$ and $t > b)$. The equations (4)–(6) thus describe a classical point moving under the influence of a constant repulsive potential Eq^2, corrected by an attractive term $-V(t)q^2$. For $E < 0$, the typical trajectory tends to $\pm\infty$ as $t \to \pm\infty$ (for large $|t|$ the repulsive force dominates, driving the classical point to infinity). Occasionally, however, a curious dynamical phenomenon occurs; some trajectories, emerging from the phase space origin ($q = p = 0$) at $t = -\infty$, by a rare coincidence, acquire a momentum sufficient to return asymptotically to the origin,

against the repulsive forces. This phenomenon, extremally unstable, represents precisely the eigenvectors of (1) [$\psi(x) \to 0$ as $x \to \pm\infty$], i.e. the most stable forms of quantum motion. The effect looks like a classical game of skill, where the 'goal' is to collocate the material point at the repulsion centre (see works on the shooting method [18]). To explain its bifurcation mechanism some geometry elements on the phase plane $\mathcal{P}$ are useful.

Due to the linearity of (4)–(5) the phase vector $q(t)$ at any $t \in \mathbf{R}$ depends linearly on the initial vector $q(a)$ for any $a \in \mathbf{R}$, i.e.

$$q(t) = u(t, a)q(a) \tag{7}$$

where the 2×2 simplectic real matrix $u(t, a)$ is called the *transference* or *evolution matrix*. Equations (4) translate themselves easily into the first order matrix equation for $u(t, a)$:

$$\frac{\mathrm{d}u}{\mathrm{d}t} = \Lambda(t)u(t, a) \tag{8}$$

where

$$\Lambda(t) = \left\| \begin{matrix} 0 & 1 \\ 2[V(t) - E] & 0 \end{matrix} \right\|. \tag{9}$$

Mathematically, the matrix equation (8)–(9) is neither easier nor more difficult to solve than the original Schrödinger equation (1). Yet it leads to geometric pictures which help to solve the spectral problem (1).

Consider first of all the region outside the potential well, $\Omega = (-\infty, a) \cup (b, +\infty)$, where $V(t) \equiv 0$. The generator $\Lambda(t)$ in Ω is constant:

$$\Lambda(t) \equiv \Lambda = \left\| \begin{matrix} 0 & 1 \\ 2|E| & 0 \end{matrix} \right\| \qquad \text{for } t \leqslant a \text{ or } t \geqslant b \tag{10}$$

leading to the explicit solutions

$$q(t) = \begin{cases} \mathrm{e}^{\Lambda(t-a)}q(a) & \text{for } t \leqslant a \\ \mathrm{e}^{\Lambda(t-b)}q(b) & \text{for } t \geqslant b. \end{cases} \tag{11}$$

Note that Λ fulfils

$$\Lambda^2 = 2|E|\mathbf{1} \tag{12}$$

and so it has two eigenvalues $\lambda_\pm = \pm\sqrt{2|E|}$ and eigenvectors $e_\pm$:

$$\begin{array}{cc} \text{eigenvalues} & \text{eigenvectors} \\ \lambda_+ = +\sqrt{2|E|} & e_+ = \left\| \begin{matrix} 1 \\ +\sqrt{2|E|} \end{matrix} \right\| \\ \lambda_- = -\sqrt{2|E|} & e_- = \left\| \begin{matrix} 1 \\ -\sqrt{2|E|} \end{matrix} \right\|. \end{array} \tag{13}$$

Henceforth, for $t \in \Omega$ (i.e. in absence of $V(t)$) the motion on the phase plane $\mathcal{P}$ preserves the directions $e_\pm$ producing a continuous squeezing: the direction e_+ expands while e_- exponentially shrinks as $t \to +\infty$ (inversely for $t \to -\infty$). In the interval $[a, b]$ this squeezing is corrected by the rotation generated by $V(t)$. (The squeezing is typically induced by the Hamiltonians of repulsive oscillators, while the attractive ones generate the phase space rotations.)

The phase trajectory (6)–(7), in general, diverges in both $+\infty$ and $-\infty$. However, exceptions exist. If the initial phase vector $q(a)$ is proportional to e_+, then in agreement with (11) $q(t)$ vanishes as $\exp[(t - a)\sqrt{2|E|}]$ for $t \to -\infty$. In turn, if $q(b)$ is proportional to e_-, then $q(t)$ vanishes as $\exp[-(t - b)\sqrt{2|E|}]$ for $t \to +\infty$. A number $E < 0$ is

an *eigenvalue* of the Schrödinger operator in (1) iff there exists a non-trivial trajectory vanishing *on both extremes* $t \to -\infty$ and $t \to +\infty$. This can happen if and only if the evolution between $t = a$ and $t = b$ brings e_+ into a vector proportional to e_-, i.e.

$$u(b, a)e_+ = \text{constant} \times e_-. \tag{14}$$

To monitor the phenomenon, consider the integral trajectories of (4)–(5) for different values of $E < 0$ (or alternatively, for different amplitudes of $V(t)$). Let I_+, I_-, $-I_+$, $-I_-$ be the radial $\frac{1}{2}$-lines determined by e_+, e_-, $-e_+$, $-e_-$ and let $\mathcal{P}^+$ and $\mathcal{P}^-$ denote two open $\frac{1}{2}$-planes limited by $\pm I_-$ containing I_+ and $-I_+$, respectively (see figure 1). In the absence of $V(t)$, $\mathcal{P}^+$ and $\mathcal{P}^-$ are evolution-invariant; as $t \to +\infty$, all the trajectories in $\mathcal{P}^+$ escape to infinity tending asymptotically to the I_+-axis while all the trajectories in $\mathcal{P}^-$ tend to $-I_+$. Consider now the trajectory which departs from $\boldsymbol{q}(-\infty) = \boldsymbol{0}$ passing through $\boldsymbol{q}(a) = e_+(E)$. If $V \equiv 0$, $\boldsymbol{q}(t) = \exp[(t-a)\sqrt{2|E|}]e_+$ (i.e. our trajectory escapes to infinity exactly along the I_+-axis). If $|V(t)|$ is non-zero but small in $[a, b]$, the escape along I_+ (due to the squeezing/expansion) is corrected by $-V(t)q^2$ which generates a clockwise rotation in $\mathcal{P}$. Yet once the rotation dies out at $t \geqslant b$, the squeezing takes over and drives the trajectory back again to I_+ as $t \to +\infty$. If $|V(t)|$ is stronger (or alternatively, if $|E|$ is weaker) the trajectory will deviate more from I_+ and return to it more slowly (figure 1). Finally, for sufficiently small $|E|$ (or sufficiently strong $|V|$), the rotation caused by $V(t)$ will bring $\boldsymbol{q}(b)$ to I_- (see figure 1). Instead of returning to I_+, the phase point will fall down right to the origin along the (shrinking) direction I_-, drawing a (normalized) eigenvector of (1). For $|E|$
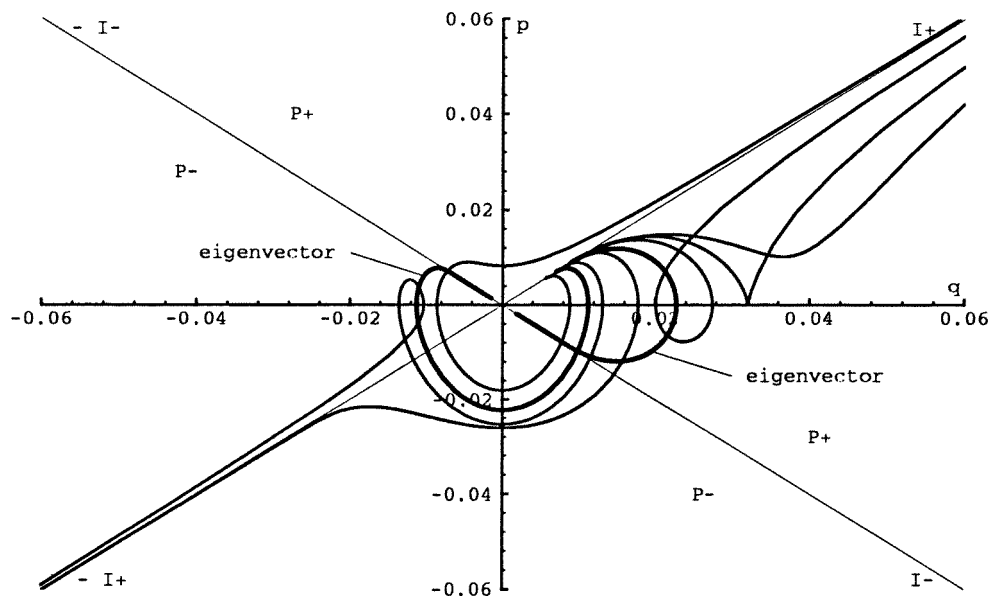

Figure 1. The metamorphosis of the classical trajectory (4)–(5) illustrates a wider concept of the spectrum, not necessarily restricted to the linear operators. We have taken $E = -\frac{1}{2}$ and $V(t)$ in the form of a 'cosinusoidal well', $V(t) = -\lambda \cos t (\lambda > 0)$ for $|t| \leqslant \pi/2$, and $V(t) \equiv 0$ for $|t| > \pi/2$. As λ grows, the deformation due to the rotating term $-V(t)q^2$ expands clockwise around the phase space origin, crossing the 'shrinking axis' $I_-(E)$ several times. At each new intersection a bifurcation occurs, producing a new closed orbit interpretable as an eigenvector of the Schrödinger equation (1). The analogous trajectory transformations would occur for a fixed $\lambda > 0$ and variable E.
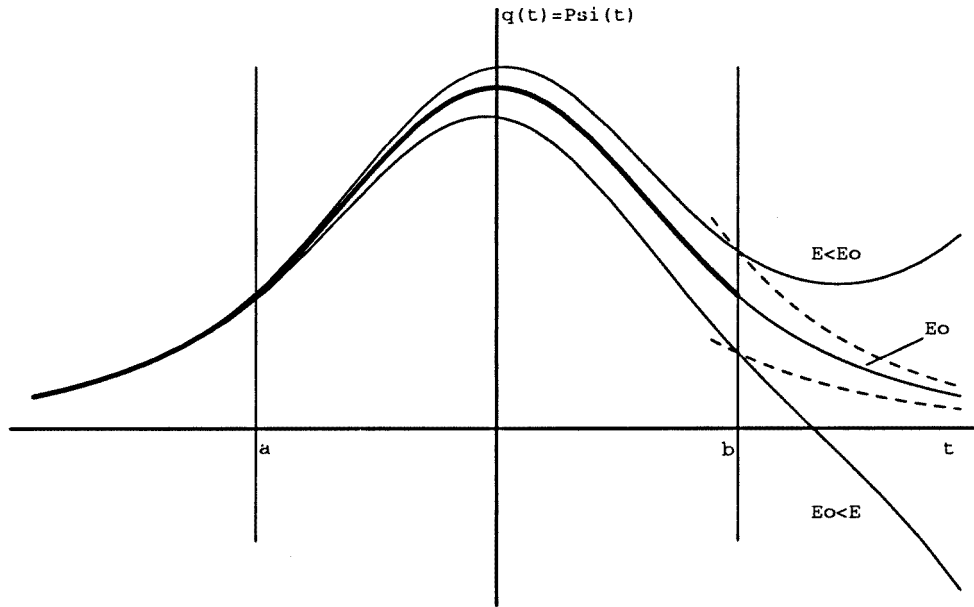
Figure 2. As $q(t)$ draws the phase trajectory (figure 1), $q(t)$ reproduces the wavefunction. Above, three cases of wavefunctions of figure 1: (i) for $E = E_0$ (the energy of the ground state) the trajectory calculated as the prolongation of the left vanishing cue at $a = -\pi/2$ achieves a smooth union with the (algebraically determined) right cue at $b = +\pi/2$; (ii) the analogous trajectory determined for $E < E_0$ fails to fit smoothly the 'right cue'. The failure produces the defect angle Γ between the numerical solution and the 'algebraic cue'; (iii) an analogous phenomenon for $E > E_0$. In both cases (ii), (iii) the defect angle Γ causes a quick divergence of $q(t)$. The same phenomenon occurs for unlimited wells; the only difference is that the cues are not exactly exponential but are given by the Riccati ansatz (2)–(3) (see appendix).

still smaller, $q(b)$ will cross to $\mathcal{P}^-$ and the trajectory will alter its asymptotic behaviour: it will tend now to $-I_+$ as $t \to +\infty$. For $|E|$ further decreasing (or $|V|$ increasing), $q(b)$ will circulate on $\mathcal{P}$ crossing subsequently $-I_-, I_-, -I_-, I_-, \ldots$. Every such event will produce a closed trajectory (an eigenvector!), coinciding with an abrupt change of the asymptotic type. The eigenvalues of the energy operator are thus interpretable as *bifurcation values* (i.e. the values of E for which the classical orbits produce bifurcations). An idea arises that the discrete spectrum of (1) could be simply *defined as a bifurcation phenomenon* caused by an 'antagonity' between two different types of motion. Such a definition would not require linear spaces, and so could be extended to the non-linear operators (see the discussions in [19]).

What is no less interesting, the *bifurcation values* can be determined by a *rather* simple algorithm, *independent of the traditional perturbation methods*.

4. The angular Riccati equations

Since the vector norms in (14) are irrelevant, (14) can be conveniently written in terms of an *angular coordinate*. Following Prüfer [3], we introduce

$$q = \rho \cos \alpha \qquad p = \rho \sin \alpha. \tag{15}$$

The canonical equations become

$$\dot{\rho}\cos\alpha - \dot{\alpha}\rho\sin\alpha = \rho\sin\alpha \tag{16}$$

$$\dot{\rho}\sin\alpha + \dot{\alpha}\rho\cos\alpha = 2[V(t) - E]\rho\cos\alpha \tag{17}$$

where $\dot{\rho}$ and $\dot{\alpha}$ mean the time derivatives. Curiously, the equation for the angular variable separates. Multiplying (16) by $-\sin\alpha$, (17) by $\cos\alpha$ (or vice versa) and adding one gets the first-order differential equation for α alone:

$$\dot{\alpha} = 2[V(t) - E]\cos^2\alpha - \sin^2\alpha \tag{18}$$

and simultaneously

$$\dot{\rho}/\rho = [V(t) - E + \tfrac{1}{2}]\sin 2\alpha. \tag{19}$$

The equation (18) was first derived by Prüfer [3], then by Drukarev [5] and Franchetti [6]. Its link to the original Ricatti idea is immediate. In fact, (18) implies

$$\frac{\mathrm{d}}{\mathrm{d}t}\tan\alpha + \tan^2\alpha = 2[V(t) - E]. \tag{20}$$

The advantages of (18) over the traditional Riccati equation (3), however, are that: (i) equation (18) can be solved for arbitrary αs without leading to singularities; (ii) it offers a clear geometric idea of the spectral condition, and (iii) it leads to an easy numerical algorithm. Indeed, notice that the phase vectors $e_{\pm}$ define the angles

$$\alpha_{\pm}(E) = \pm\arctan\sqrt{2|E|} \tag{21}$$

$$\delta(E) = \alpha_{+}(E) - \alpha_{-}(E) = 2\arctan\sqrt{2|E|}. \tag{22}$$

In agreement with (11), the trajectory tends to zero in $-\infty$ iff $\alpha(a) = \alpha_{+} + k\pi$, and it tends to zero in $+\infty$ iff $\alpha(b) = \alpha_{-} + m\pi$. The trajectory tends to zero for both $t \to \pm\infty$ iff the time evolution (18) converts the initial angle $\alpha(a) = \alpha_{+}$ into $\alpha(b) = \alpha_{-} \pm n\pi$. Thus, to check whether a number $E < 0$ is an energy eigenvalue it is sufficient to solve the differential equation (18) with E fixed and with the initial condition $\alpha(a) = \alpha_{+}(E)$, finding $\alpha(b) = \alpha(b, E)$. Whenever the total angular change $\Delta\alpha = \alpha(a) - \alpha(b)$ in $[a, b]$ fulfils

$$\Delta\alpha = \delta(E) + n\pi \qquad n = 0, 1, 2, \ldots \tag{23}$$

E belongs to the discrete spectrum. A convenient form of (23) involves the *spectral defect angle* defined as a difference between the *desired angle* $\alpha_{-}(E)$ and the *achieved angle* $\alpha(b, E)$:

$$\Gamma(E) = \alpha_{-}(E) - \alpha(b, E) = \Delta\alpha - \delta(E). \tag{24}$$

The condition (23) then tells

$$\Gamma(E) = n\pi \qquad n = 0, 1, 2, \ldots. \tag{25}$$

An immediate generalization of the conditions (23)–(25) is obtained for $V(t)$ constant but not necessarily vanishing outside (a, b):

$$V(t) = \begin{cases} V(a) & \text{for } t \leqslant a \\ V(b) & \text{for } t \geqslant b. \end{cases} \tag{26}$$

The motion (4)–(6) then has two different constant generators $\Lambda(a)$ and $\Lambda(b)$ for $t \leqslant a$ and $t \geqslant b$ and the formulae (23)–(25) hold after substituting $|V(a) - E|$ or $|V(b) - E|$ instead of $|E|$ in the expression (21) for α_{+} and α_{-}, respectively.

Observe that (15) is not the only way to separate the angular part of (4). The $\mathcal{P}$-plane is a simplectic space without a natural measure of distances and angles. Henceforth, instead

of introducing the polar variable (15) straightforwardly, one might as well introduce new canonical coordinates q', p', and only after define the angular variable on q', p' plane. Some profits of this freedom were explored by Calogero [12]; here let us notice only the plausible form of the spectral condition if the new angular variable is introduced by

$$q = \kappa \rho \cos \gamma$$
$$p = \kappa^{-1} \rho \sin \gamma \tag{27}$$

where $\kappa = (2|E|)^{-1/4}$. The motion equations then read

$$\dot{\gamma} = \sqrt{2|E|} \cos 2\gamma + \sqrt{2/|E|} V(t) \cos^2 \gamma \tag{28}$$

$$\dot{\rho}/\rho = \left(\sqrt{2|E|} + V(t)\sqrt{|E|/2} \right) \sin 2\gamma \tag{29}$$

and the limiting angles are independent of $E (\gamma_\pm = \pm \frac{\pi}{4})$. The spectral condition becomes

$$\Delta \gamma = (n + \tfrac{1}{2})\pi \tag{30}$$

in a visible reconciliation between the oscillator spectrum and the Sommerfeld quantization conditions.

5. The numerical algorithm

The importance of the angular variables, in principle, has been known for a long time [3–6, 12, 13, 20]. The *defect angle* equivalent to (24) was introduced by Calogero, to evaluate the number of the energy levels for the one-dimensional and radial Schrödinger eigenproblem [13]. Yet, the efficiency of the method to determine the exact eigenvalues somehow escaped attention (perhaps due to a general fascination with the perturbative methods!). The first reason why (18) is so easily applicable is:

Theorem 1. For any bounded, piece-wise continuous $V(t)$ with a compact support in $[a, b]$, $\Gamma(E)$ is a strictly increasing function of E for $E < \min\{V(a), V(b)\}$.

The proof is deduced from two observations. (i) If $\alpha(t)$ and $\alpha'(t)$ are two solutions of (18) with $\alpha(a) < \alpha'(a)$ then $\alpha(b) < \alpha'(b)$ (indeed, otherwise there would be a point $c \in [a, b]$ with $\alpha(c) = \alpha'(c)$ contradicting the uniqueness of the solutions of (18)); (ii) if $\alpha_1(t)$ and $\alpha_2(t)$ are solutions of two equations of form (18) with two different parameters $E = E_1$ and $E = E_2$, respectively, and $E_1 > E_2$, then $\alpha_1(a) = \alpha_2(a) \Rightarrow \alpha_1(b) < \alpha_2(b)$ (the proof involves only the standard comparison theorem for equation (18); see e.g. [21], p 394). The observations (i) and (ii) imply now that $\alpha(b, E)$ for an angular trajectory starting in $\alpha(a) = \alpha_+(E)$ is a monotonically decreasing function of E, and the proof is completed by noticing that $\alpha_-(E)$ is increasing.

As an illustration, we have used (25) to determine the energy levels for the truncated one-dimensional oscillator potential (see also [22]):

$$V(x) = \begin{cases} \frac{1}{2}\omega^2 x^2 & \text{for } |x| \leqslant a \\ \frac{1}{2}\omega^2 a^2 & \text{for } |x| \geqslant a. \end{cases} \tag{31}$$

The limiting angles are $\alpha_\pm = \pm \arctan \sqrt{w^2 a^2 - 2E}$. We have determined the angular function $\Gamma(E)$, $0 < E < V(a)$, for $w = 1$, $a = 2$ and $a = 4$, by integrating numerically the angular equation (18) (see figure 3). It yields the two energy levels for the oscillator truncated at $a = 2$, and eight energy levels for the oscillator truncated at $a = 4$, all calculated with accuracy up to 10^{-10}. Curiously, the obtained eigenvalues are very close to the first two and eight levels of the exact oscillator, respectively, $E_n = n + \frac{1}{2}$ (indeed, even the last
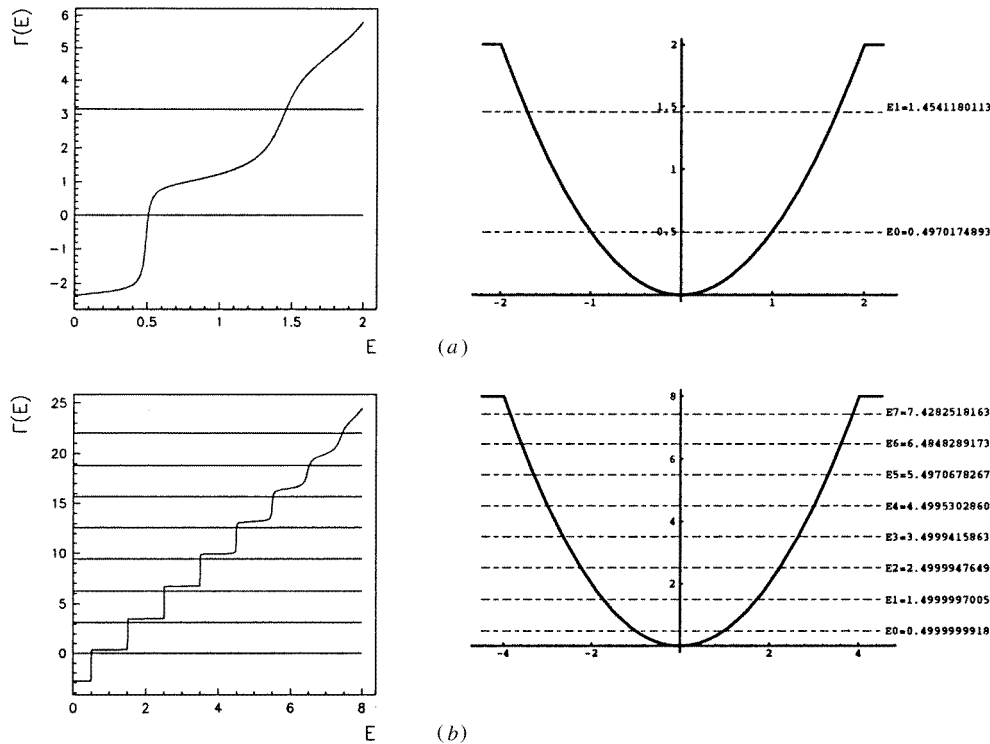
Figure 3. The defect angle $\Gamma(E) = \alpha_- - \alpha(a, E)$ for two cases of truncated oscillators: (*a*) $b = -a = 2$ and (*b*) $b = -a = 4$. The intersections of the 'stepping' functions $\Gamma(E)$ with the horizontal lines $\Gamma = n\pi$ give the eigenvalues of the Schrödinger problem.

eigenvalues of the truncated potential (31) differ very little from the orthodox $E_1 = 1.5$, and $E_7 = 7.5$). Compared with the Ritz method, the basic advantage of our algorithm is its essential simplicity (no need to waste skills inventing an adequate class of test functions). A notable advantage (and this is the second reason why (18) is so easily applicable) is that the spectral function $\Gamma(E)$ is *unstable* and changes very quickly when crossing the sequence of critical values $\Gamma = n\pi (n = 1, 2, \ldots)$ (see figure 3). Thus, even a very small change of E in the vicinity of an eigenvalue, translates into a visible effect in Γ, significantly improving the accuracy. This 'smashing error effect' was apparently overlooked when the angular algorithms were formulated [3–6]. It is explained by the fact that the energy eigenvalues correspond to the bifurcations of the orbits and the final point $\alpha(b)$ deflects very fast when E crosses the bifurcation value (compare Calogero [23], p 274). In the limit as $b = +\infty$, $\alpha(b, E)$ would be discontinuous and $\Gamma(E)$ would be an exact step function!

6. The '$\frac{1}{2}$ eigenproblem'

The method, until now, concerns only the potentials constant outside finite intervals (limited, non-singular wells). Could it tell us something about more general $V(t)$? Consider any continuous $V : \mathbf{R} \to \mathbf{R}$ such that:

$$V_\pm = \liminf_{t \to \pm\infty} V(t) > -\infty. \tag{32}$$

In the traditional approach to the spectral problem, the main effort is to find the non-trivial solutions of (1) vanishing on both extremes $t \to \pm\infty$ (which exists only as an exception!) Following the observations of section 5 we propose to reduce the solution to two minor steps, each one interpretable as a '$\frac{1}{2}$ spectral problem': (i) for any E find the special solutions of (1) which vanish for $t \to -\infty$ (the 'left eigenvectors'); (ii) find the solutions of (1) which vanish for $t \to +\infty$ (the 'right eigenvectors').

While the difficulty of solving the complete spectral problem is formidable, one seldom pays attention to the fact that every 'half of it' has a solution *always*, defining some *left (right) decaying branches* for (1) for any $E < V_-(E < V_+)$. For big $|t|$ they provide the *asymptotic cues* $e_\pm(t, E)$ and *asymptotic angles* $\alpha_\pm(t, E)$ adequate to replace the fixed vectors $e_\pm(E)$ (13) and *angles* $\alpha_\pm(E)$ in the algorithm of section 5. Indeed, one has:

Lemma A. Let $\beta : \mathbf{R} \to \mathbf{R}$ be a continuous real function with

$$\liminf_{t \to +\infty} \beta(t) > \eta^2 > 0. \tag{33}$$

Then the two-dimensional solution space Ξ of the second-order differential equation

$$\frac{\mathrm{d}^2 q}{\mathrm{d}t^2} = \beta(t)q(t) \tag{34}$$

has a one-dimensional subspace Ξ_- of solutions which vanish for $t \to +\infty$ and are square integrable in $[0, +\infty)$.

Proof. Let N be a number such that $\beta(t) > \eta^2$ for $t \geqslant N$. For $t \geqslant N$, the material point $q(t)$ moves under the influence of the repulsive elastic force

$$\ddot{q} \geqslant \eta^2 q. \tag{35}$$

Consider now an integral trajectory of (33) which satisfies the initial condition: $q(N) = C > 0$, $\dot{q}(N) = \eta C > 0$. Using (35) one easily shows that $q(t)$ is positive, monotonically increasing and

$$q(t) \geqslant q(N)\mathrm{e}^{\eta(t-N)} = K\mathrm{e}^{\eta t}. \tag{36}$$

The method of the variation of constant then provides a new, linearly independent solution:

$$q_-(t) = q(t) \int_t^{+\infty} \frac{\mathrm{d}\tau}{q(\tau)^2} \leqslant q(t) \int_t^{+\infty} \frac{\mathrm{d}\tau}{q(t)q(\tau)} = \int_t^{+\infty} \frac{\mathrm{d}\tau}{q(\tau)} \leqslant \frac{\mathrm{e}^{-\eta t}}{C\eta} \tag{37}$$

which spans the desired subspace Ξ_-. $\square$

An immediate consequence is:

Theorem 2. Let $V(t)$ be a continuous potential in the one-dimensional Schrödinger equation (1) and assume (32) holds. Then for every $E < V_-$, the two-dimensional solution space of (1) contains a one-dimensional subspace $\Xi_+(E)$ of solutions vanishing for $t \to -\infty$, square integrable in $(-\infty, 0]$, while for any $E < V_+$ it contains a one-dimensional subspace $\Xi_-(E)$ of solutions vanishing for $t \to +\infty$, square integrable in $[0, +\infty)$. A number $E < \min(V_-, V_+)$ is a point of the discrete spectrum of (1) if the subspaces $\Xi_-(E)$ and $\Xi_+(E)$ coincide.

Proof. The proof is obtained by applying lemma A to t and $-t$ with $\beta(t) = V(t) - E$ and $0 < \eta^2 < V_\pm - E$ respectively.

In the appendix we have collected the asymptotic forms of both 'decaying branches' of (1) for several $V(t)$ including the oscillator and Coulomb potentials (see appendix). These cues (the '$\frac{1}{2}$-eigenvectors') permit us to solve, with any desired accuracy, the traditional

spectral problem for a class of infinite potential wells. Let $V(t)$ be one of these potentials and let $\bar{E} < V_\infty$. The energy eigenvalues $E < \bar{E}$ (if they exist), can then be determined by the following algorithm, generalizing the one of section 5:

(i) one fixes a finite interval $[a, b] \subseteq \mathbf{R}$ such that $V(t) - \bar{E}_0 \geqslant \kappa > 0$ and the asymptotic cue expressions are valid for $t \leqslant a$ and $t \leqslant b$;

(ii) one uses the 'vanishing cues' $q_\pm(t, E)$ to define two special angles

$$\alpha_-(a, E) = \arctan[p_-(a, E)/q_-(a, E)] \tag{38}$$

$$\alpha_+(b, E) = \arctan[p_+(b, E)/q_+(b, E)] \tag{39}$$

characteristic for the trajectories vanishing at $t \to -\infty$ and $t \to +\infty$;

(iii) one integrates the equation (18) in $[a, b]$ with the initial condition $\alpha(a) = \alpha_+(a, E)$ finding $\alpha(b) = \alpha(b, E)$ and determining the *defect angle*

$$\Gamma(E) = \alpha_-(b, E) - \alpha(b, E) \tag{40}$$

(iv) whenever

$$\Gamma(E) = n\pi \qquad n = 0, 1, 2, \ldots \tag{41}$$

the number $E < \bar{E}$ belongs to the point spectrum of the Schrödinger operator.

The non-trivial part of the method, of course, is to find the vanishing cues [24]. However, as the interval $[a, b]$ can be arbitrarily wide, it is enough to know the asymptotic expressions. Now, if (32) holds and $E < \bar{E}$, the cues are monotonic, without zeros for $t < a$ and $t > b$; one can thus use the ansatz (2)–(3). Note that while the general solution f of the Riccati equation (3) depends on one arbitrary constant, and (typically) diverges as $t \to \pm\infty$, the $f(t)$ of *vanishing cue* has no such arbitrariness, and can be determined with any desired accuracy by applying the known iterative or asymptotic methods (see appendix). For the oscillator and Coulomb potentials the cues ('$\frac{1}{2}$-eigenvectors') are already known in the form of the asymptotic series for the confluent hypergeometric equation, vanishing either at $t \to 0_+$ or $t \to \infty$ (however, we prefer to represent them in the form $q(t) = \exp\{f(t)\}$, since $f(t) = \tan\alpha$ defines the asymptotic angles).

Once the cues $q_\pm$ (and the angles $\alpha_\pm$) are determined, they can be used not only to find the spectrum for one particular potential $V(t)$ but simultaneously, for an entire class of potentials which share the asymptotical behaviour of $V(t)$ (and can be arbitrarily deformed in any finite region). Moreover, given the 'left cues' for one potential $V_1(t)$ and the 'right cues' for another potential $V_2(t)$ the method can be used as well to determine the spectrum of any $V(t)$ sharing the asymptotic behaviour of $V_1(t)$ for $t \to -\infty$ and of $V_2(t)$ for $t \to +\infty$.

For curiosity, we have used the asymptotic angles calculated in our appendix to determine the spectrum for the 'hybrid oscillator' (figure 4) not so easily treatable by either perturbative or variational methods:

$$V(x) = \begin{cases} \frac{1}{2}x^2 & \text{for } x \geqslant 0 \\ \frac{1}{8}x^2 & \text{for } x \leqslant 0. \end{cases} \tag{42}$$

For the operation interval $[a, b] = [-50, 50]$ the limiting angles were found by using the first five terms of the 'Riccati series' for $f(t)$ (appendix). The computer was then asked to integrate equation (18) by the Runge–Kutta method with accuracy and precision goals 10^{-10} determining $\Gamma(E)$ for a sequence of Es and solving (25) by interpolation. An identical method applied to the genuine oscillator yields E_0, E_1 with the first nine decimals, and E_2, E_3 with eight decimals correct.

Note that our method permits us to solve as easily any other hybrid or deformed cases (as for example an oscillator affected by an arbitrarily high potential barrier in the middle, etc).
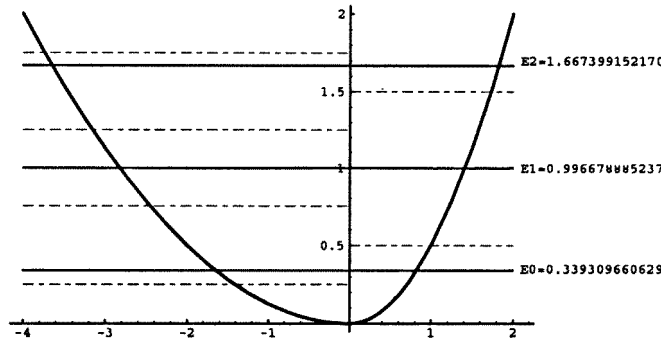
Figure 4. The hybrid oscillator potential. The broken lines represent the standard energy eigenvalues for each separated oscillator, and the full lines represent the actual eigenvalues for this potential.

7. Singular and radial wells

The physically important wells not only extend to infinity, but can have singularities in the finite region. The typical case is the one-dimensional equation (1) obtained after separation of the angular variables in the Schrödinger equation in $\mathbf{R}^3$ with a radial potential $\phi(r)$. By denoting $\psi(\boldsymbol{x}) = R(r)Y(\theta, \phi)$ and assuming $Y(\theta, \phi)$ to be an eigenfunction of the square angular momentum $\boldsymbol{L}^2$, one ends up with the one-dimensional eigenvalue problem for $u(t) = tR(t)$:

$$-\frac{\mathrm{d}^2 u}{\mathrm{d}t^2} + \left[2V(t) + \frac{l(l+1)}{t^2} - 2E \right] u = 0 \tag{43}$$

whose eigenvectors are the trajectories vanishing for $t \to 0_+$ and square integrable in any $[b, +\infty)(b > 0)$. Similarly as before, each of the asymptotical conditions, typically, can be satisfied by solutions of (1) for any E. The existence of the *right cues* (solutions vanishing for $t \to +\infty$) is assured by theorem 2. In turn, the existence of the *zero-cues* (solutions vanishing at 0_+) is the consequence of the following elementary theorem:

Theorem 3. Let $\phi(t)$ be a continuous real function in $(0, +\infty)$, satisfying

$$\phi(t) \geqslant -k(t) \tag{44}$$

in a certain subinterval $(0, \delta > 0)$, where $k : (0, \delta) \to \mathbf{R}$ fulfils

$$k(t) \geqslant 0 \qquad \text{and} \qquad \int_0^\delta \int_t^\delta k(t') \, \mathrm{d}t' < +\infty. \tag{45}$$

Then the two-dimensional space Ξ of the functions $u : (0, +\infty) \to \mathbf{R}$ which solve the second-order differential equation

$$-\frac{\mathrm{d}^2 u}{\mathrm{d}t^2} + \phi(t)u = 0 \tag{46}$$

must contain a one-dimensional subspace Ξ_0 of solutions which vanish for $t \to 0_+$.

Proof. We shall stick to the classical image of section 2 putting $u(t) = q$ and $\dot{u}(t) = p$; (46) then paint the motion of a classical point mass $m = 1$ under the influence of the elastic force $-2\phi(t)q(t)$. Choose now $a \in (0, \delta)$ such that

$$K(a) = \int_0^a \int_t^a k(t') \, \mathrm{d}t' \, \mathrm{d}t < 1. \tag{47}$$

We shall first of all prove the following lemma:

Lemma B. If $(\theta, b] \subset (0, a]$, if $q(t)$ is a solution of (46) with $\dot{q}(b) = 0$ and if $0 \leqslant q(t) \leqslant q(b)$ for all $t \in (\theta, b]$, then also

$$q(t) \geqslant [1 - K(a)]q(b) \tag{48}$$

for $t \in (\theta, b]$.

In fact, the assumptions (44)–(45) subsequently imply

$$\ddot{q}(t) \geqslant -k(t)q(t) \Rightarrow \tag{49}$$

$$\Rightarrow \dot{q}(b) - \dot{q}(t) = \int_t^b \ddot{q}(t')\,dt' \geqslant -\int_t^b k(t')q(t')\,dt' \geqslant -q(b)\int_t^b k(t')\,dt' \Rightarrow \tag{50}$$

$$\Rightarrow \dot{q}(t) \leqslant q(b)\int_t^b k(t')\,dt' \Rightarrow \tag{51}$$

$$\Rightarrow q(b) - q(t) = \int_t^b \dot{q}(t')\,dt' \leqslant q(b)\int_t^b \int_{t'}^b k(t'')\,dt''\,dt' \leqslant K(a)q(b) \Rightarrow \tag{52}$$

$$\Rightarrow q(t) \geqslant [1 - K(a)]q(b). \tag{53}$$

Consider now any solution $q(t)$ of (46) with

$$q(a) > 0 \qquad \dot{q}(a) = 0. \tag{54}$$

We shall show that

$$\kappa = \inf_{t \in (0,a)} q(t) > 0. \tag{55}$$

Suppose, to the contrary, that $\kappa \leqslant 0$. Then $q(t)$ either vanishes at some $\theta \in (0, a)$ or vanishes in limit at $\theta = 0$. In either case

$$\lim_{t \to \theta_+} q(t) = 0 \qquad (0 \leqslant \theta < a) \tag{56}$$

and so $q(t)$ is bounded in $(\theta, a]$. Denote $\bar{q} = \sup_{t \in (0,a]} q(t) \geqslant q(a) > 0$. Since $q(t)$ is continuous in $(0, a]$ it must accept the value $\bar{q}$ at some point b, $\theta < b \leqslant a$. If $b < a$, then $q(t)$ has a local maximum at b and $\dot{q}(b) = 0$. If $b = a$, then also $\dot{q}(b) = \dot{q}(a) = 0$ because of (54). Our lemma henceforth implies (48) for all $t \in (\theta, b]$ contradicting (56) and making $\kappa \leqslant 0$ impossible to sustain. We have thus shown (55). Now, the standard method of the 'variation of constant' provides the new solution of (46):

$$q_0(t) = q(t)\int_0^t \frac{d\tau}{q(\tau)^2} \tag{57}$$

where $h(t) = 1/q(t)$ due to (49) is positive and bounded in $(0, a)$. It remains to prove that $q_0(t) \to_{t \to 0_+} 0$. Choose any $t, \tau, 0 < \tau \leqslant t \leqslant a$. We shall show that

$$q(\tau) \geqslant [1 - K(a)]q(t). \tag{58}$$

In fact, suppose first of all that $q(\tau) \geqslant q(t)$; then (58) trivially holds. Suppose in turn that for some $\tau \in (0, t)$, $q(\tau) < q(t)$. Then there must be a point $b' \geqslant \tau$ in which q accepts its upper limit in $[\tau, a] \Rightarrow q(b') > q(t)$, $\dot{q}(b') = 0$, and our lemma immediately implies

$$q(\tau) \geqslant [1 - K(a)]q(b') \geqslant [1 - K(a)]q(t). \tag{59}$$

Inserting this to (57), one has

$$q_0(t) = q(t)\int_0^t \frac{d\tau}{q(\tau)^2} \leqslant q(t)\int_0^t \frac{d\tau}{q(t)^2[1 - K(a)]^2}$$

$$\leqslant \frac{1}{q(t)}t\frac{1}{[1 - K(a)]^2} \leqslant t\frac{1}{\kappa[1 - K(a)]^2} \to_{t \to 0_+} 0. \tag{60}$$

$\square$

In the appendix we have collected examples of asymptotic cues at 0^+ for some typical singularities.

To check the results, we have used the right cues ($t \to +\infty$) and the zero-cues of the appendix to determine the discrete spectrum for the Coulomb well $V(t) = -\frac{1}{t}$. Without any advanced techniques of the shooting method [18], we have solved the angular equation (18) with the help of the standard package 'Mathematica' (which uses the Runge–Kutta method), obtaining the first 10 levels of the hydrogen atom.

$$E_0 = -0.500\,000\,000\,0$$
$$E_1 = -0.125\,000\,000\,0$$
$$E_2 = -0.055\,555\,555\,5$$
$$E_3 = -0.031\,249\,999\,9$$
$$E_4 = -0.020\,000\,000\,0$$
$$E_5 = -0.013\,888\,888\,8$$
$$E_6 = -0.010\,204\,081\,6$$
$$E_7 = -0.007\,812\,500\,0$$
$$E_8 = -0.006\,172\,839\,5$$
$$E_9 = -0.005\,000\,000\,0$$

The unexpectedly good accuracy to 10^{-10} for such a simple procedure is explained by the fact that: (i) equation (18) is of the first order, and (ii) by the instability phenomenon (the 'error annihilating effect' noticed in section 5). Once the asymptotic expressions were cross-examined, we used the already tested right cues of the oscillator and the 0_+ cues of the Coulomb singularity to find the principal series of energy levels for the 'hybrid well':

$$V(r) = -\frac{1}{r} + \frac{1}{2}w^2 r^2 \tag{61}$$

sometimes considered as a candidate to describe the quark confinement [25]. Taking $w^2 = 0.000\,05$ we could observe that a very weak oscillator potential cancels the condensation of the hydrogen energy levels for $E \to 0^-$, providing a continuous transition to an equally spaced spectrum for $E > -0.01$ (see figure 4). Let us also notice that a close relative of our method has been successfully used to study the logarithmic wells [26].
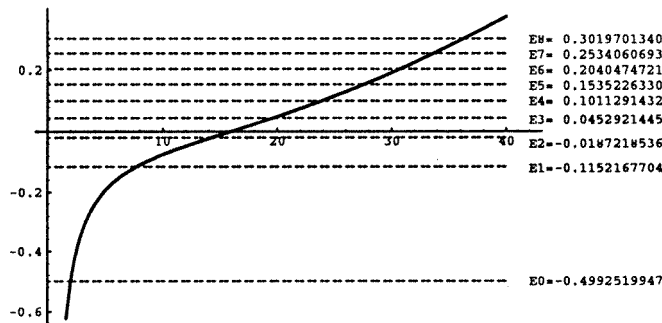

Figure 5. A hybrid well: the kind which could resemble the quark confinement.

We are tempted to predict that in the not-too-distant future, the perturbative methods of determining spectra (at least for the one-dimensional Schrödinger operator) will be almost forgotten and a part of patience nowadays devoted to special functions (permitting us to

solve only exceptional problems!) will be invested into building up a bank of data about the asymptotic behaviours and 'vanishing cues'. Once these data are precise enough, the task of determining the spectra of arbitrary potentials of known asymptotic types will become a question for pocket calculators.

Acknowledgments

Appendix. The evaluation of the vanishing cues

Below, we look straightforwardly for $f = \tan\alpha$ defined by the Riccati equation (3) and yielding $q(t) = e^{\int f(t')\,dt'}$ which vanish either for $t \to \pm\infty$ or $t \to 0_+$.

A. Harmonic oscillator

The solution to the Riccati equation

$$\dot{f} + f^2 = w^2 t^2 - 2E$$

which yields $q(t) \to 0$ for $t \to \pm\infty$, can be found in the form of an infinite series:

$$f(t) = -wt + \sum_{i=0}^{+\infty} a_i t^{-i}$$

where

$$a_0 = a_{2s} = 0 \qquad a_1 = \frac{E}{w} - \frac{1}{2}$$

$$a_{s+1} = \frac{1}{2w}\left\{ -(s-1)a_{s-1} + \sum_{j=1}^{s} a_j a_{s-j} \right\} \qquad (s \geqslant 2).$$

Explicitly

$$f(t) = -wt + \left(\frac{E}{w} - \frac{1}{2}\right)\frac{1}{t} + \frac{1}{2w}\left(\frac{E}{w} - \frac{1}{2}\right)\left(\frac{E}{w} - \frac{3}{2}\right)\frac{1}{t^3}$$

$$+ \frac{1}{2w^2}\left(\frac{E}{w} - \frac{1}{2}\right)\left(\frac{E}{w} - \frac{3}{2}\right)\left(\frac{E}{w} - 2\right)\frac{1}{t^5} + \frac{1}{2w^3}\left(\frac{e}{w} - \frac{1}{2}\right)\left(\frac{E}{w} - \frac{3}{2}\right)$$

$$\times \left[\left(\frac{E}{w} - 2\right)\left(\frac{E}{w} - 3\right) + \frac{1}{4}\left(\frac{E}{w} - \frac{1}{2}\right)\left(\frac{E}{w} - \frac{3}{2}\right)\right]\frac{1}{t^7}$$

$$+ \frac{1}{2w^4}\left(\frac{E}{w} - \frac{1}{2}\right)\left(\frac{E}{w} - \frac{3}{2}\right)\left[\left(\frac{E}{w} - 2\right)\left(\frac{E}{w} - 3\right)\left(\frac{E}{w} - 4\right)\right.$$

$$+ \frac{1}{4}\left(\frac{E}{w} - \frac{1}{2}\right)\left(\frac{E}{w} - \frac{3}{2}\right)\left(\frac{E}{w} - 4\right)$$

$$\left. + \frac{1}{2}\left(\frac{E}{w} - \frac{1}{2}\right)\left(\frac{E}{w} - \frac{3}{2}\right)\left(\frac{E}{w} - 2\right)\right]\frac{1}{t^9} + \cdots.$$

The asymptotic form of the '$\frac{1}{2}$-eigenvectors' for $t \to \pm\infty$ is

$$q_{\mp} \simeq e^{-\frac{1}{2}wt^2}|t|^{(\frac{E}{w}-\frac{1}{2})}e^{-\frac{1}{w}(\frac{E}{w}-\frac{1}{2})(\frac{E}{w}-\frac{3}{2})[\frac{1}{t^2}+\frac{2}{w}(\frac{E}{w}-2)\frac{1}{t^4}+\cdots]}.$$

The consistency with the textbook expressions for $\psi(t)$ in terms of the confluent hypergeometric function is easily verified.

B. The Coulomb potential

The series solution for

$$\dot{f} + f^2 = -\frac{2}{t} + \frac{l(l+1)}{t^2} - 2E$$

(yielding $q_0(t) \to 0$ when $t \to 0_+$) turns out to be

$$f_0 = \frac{l+1}{t} + \sum_{i=0}^{+\infty} a_i t^i.$$

Explicitly

$$f_0 = \frac{l+1}{t} - \frac{1}{l+1} - \frac{2E(l+1)^2+1}{(2l+3)(l+1)^2}t + \cdots.$$

Henceforth, the '$\frac{1}{2}$-eigenvector' vanishing for $t \to 0_+$ is

$$q_0 \simeq t^{l+1}e^{-\frac{1}{l+1}t-\frac{2E(l+1)^2+1}{2(2l+3)(l+1)^2}t^2+\cdots}$$

consistently with the well known expressions in terms of the confluent hypergeometric series.

For $t \to +\infty$, by similar arguments, f has the form

$$f_- = -\sqrt{2|E|} + \frac{1}{\sqrt{2|E|}}\frac{1}{t} - \frac{2l(l+1)|E|+\sqrt{2|E|}-1}{4|E|\sqrt{2|E|}}\frac{1}{t^2} + \cdots$$

yielding the '$\frac{1}{2}$-eigenvector'

$$q_- \simeq e^{-\sqrt{2|E|}t}t^{\frac{1}{\sqrt{2|E|}}}e^{h(1/t)}$$

where $h(\xi)$ has the form of an analytic series vanishing at $\xi = 0$. However, we have found that if the integration interval is wide enough, a simpler asymptotic expression gives good results:

$$f_- = -\sqrt{-2E - \frac{2}{t} + \frac{l(l+1)}{t^2}}$$

and the only problem we have is to integrate the angular equation (18) in a sufficiently long range, to have the cue without nodal points. The integration can be simplified by changing variables from t to $x = t/(1+t)$.

C. The Yukawa potential

This case is very similar to the preceding one, though no longer treatable in terms of hypergeometric series. The Riccati equation for $f(t) = \tan \alpha(t)$ reads

$$\dot{f} + f^2 = -\frac{2}{t} e^{-\lambda t} + \frac{l(l+1)}{t^2} - 2E.$$

Our theorem 3 ensures the existence of the solution of (1) vanishing at zero, of the form $\psi_0(t) = \exp\{f_0(t)\}$ where

$$f_0 = \frac{l+1}{t} + \sum_{i=0}^{+\infty} a_i t^i.$$

After calculations

$$a_0 = \frac{-1}{l+1} \qquad a_1 = \frac{2(\lambda - E)(l+1)^2 - 1}{(2l+3)(l+1)^2}$$

$$a_{s+1} = \frac{-1}{2l+s+3} \left\{ \frac{2(-\lambda)^{s+1}}{(s+1)!} - \sum_{r=0}^{s} a_r a_{s-r} \right\} \qquad (s \geqslant 1).$$

Henceforth, the vanishing cue $q_0(t)$ is

$$q_0(t) \simeq t^{l+1} e^{-\frac{1}{l+1} t + \frac{2(\lambda - E)(l+1)^2 - 1}{2(2l+3)(l+1)^2} t^2 + \cdots}$$

(no longer representable in terms of the confluent hypergeometric series!).

For $t \to +\infty$, we have used a finite approximant:

$$f_- = \sqrt{\frac{l(l+1)}{t^2} - 2E - \frac{2}{t} e^{-\lambda t}}$$

changing simultaneously the integration variable to $x = t/(1+t)$.

D. A hybrid 'quark potential'

The Riccati equation (3) for the effective potential

$$V(t) = -\frac{1}{t} + \frac{1}{2} w^2 t^2 - \frac{l(l+1)}{2t^2}$$

yields the following $f_0(t)$ for $t \to 0_+$:

$$f_0 = \frac{l+1}{t} - \frac{1}{l+1} - \frac{2E(l+1)^2 + 1}{(2l+3)(l+1)^2} t - \frac{2E(l+1)^2 + 1}{(2l+3)(l+1)^3(l+2)} t^2$$

$$+ \frac{1}{2l+5} \left\{ w^2 - \frac{4E(l+1)^2 + 2}{(2l+3)(l+1)^4(l+2)} - \frac{(2E(l+1)^2 + 1)^2}{(2l+3)^2(l+1)^4} \right\} t^3 + \cdots.$$

The vanishing cue

$$q_0 = t^{l+1} e^{-\frac{1}{l+1} t + g(t)}$$

where $g(t)$ has the form of an analytical series.

Meanwhile, the solution vanishing at $t \to +\infty$ corresponds to $f_-(t)$ in the form

$$f_- = -wt + \left[\frac{E}{w} - \frac{1}{2} \right] \frac{1}{t} + \frac{1}{w} \frac{1}{t^2} + \frac{1}{2w} \left\{ \left[\frac{E}{w} - \frac{1}{2} \right] \left[\frac{E}{w} - \frac{3}{2} \right] - l(l+1) \right\} \frac{1}{t^3} + \cdots.$$

The vanishing cue is

$$q_- \simeq e^{-\frac{1}{2} w t^2} t^{\left(\frac{E}{w} - \frac{1}{2} \right)} e^{k(1/t)}$$

where $k(\xi)$ is an analytic series vanishing at $\xi = 0$.

References

[1] Plebanski J 1977 *J. Math. Phys.* **18** 2511
[2] Aharonov Y and Au C K 1979 *Phys. Rev. Lett.* **42** 1582
[3] Prüfer H 1926 *Math. Ann.* **95** 409
[4] Milne W E 1930 *Phys. Rev.* **35** 863
[5] Drukarev G F 1949 *J. Eksp. Theor. Phys.* **19** 247
[6] Francetti S 1957 *Nuovo Cimento* **6** 601
[7] See e.g. Merzbacher E 1970 *Quantum Mechanics* (New York: Wiley)
[8] Jost R and Pais A 1951 *Phys. Rev.* **82** 840
[9] Jost R and Khon W 1952 *Phys. Rev.* **87** 977
[10] Bargmann V 1952 *Proc. Natl Acad. Sci., USA* **38** 961
[11] Schwinger J 1961 *Proc. Natl Acad. Sci., USA* **47** 122
[12] Calogero F 1965 *J. Math. Phys.* **6** 161
[13] Calogero F 1965 *Commun. Math. Phys.* **1** 80
[14] Malkin I A and Man'ko V I 1970 *Sov. Phys.–JETP* **31** 386
[15] Coleman S 1985 Classical lumps and their quantum descendants *Aspects of Symmetry* (Cambridge: Cambridge University Press)
[16] Ashtekar A 1995 *Proc. CAM94* ed A Zepeda, (New York: AIP)
[17] Avron J E and Simon B 1981 *Phys. Rev. Lett.* **46** 1166
[18] Hodgson R J W 1988 *J. Phys. A: Math. Gen.* **21** 679; (1988) A **21** 1563
Killinbeck J 1987 *J. Phys. A: Math. Gen.* **20** 1411
[19] Czachor M 1994 Elements of non-linear quantum mechanics *Preprint*
[20] Newton R G 1960 *J. Math. Phys.* **1** 319
[21] Hille E 1969 *Lectures on Ordinary Differential Equations* (Reading, MA: Addison-Wesley)
[22] Mielnik B and Reyes M A 1995 Classical trajectories and quantum spectra *Talk at IV ICSSUR (Shanxi)*
[23] Calogero F 1963 *Nuovo Cimento* **27** 261
[24] Reyes M A 1992 La ecuación angular de Riccati y el problema espectral unidimensional *Master's Thesis* CINVESTAV, México
[25] López Castro G 1995 private discussion
[26] Eveker K, Grow D, Jost B, Monfort C E III, Nelson K W, Stroh C and Witt R C 1990 *Am. J. Phys.* **58** 1183